Numerical Investigation of the Unsteady Flows in a Transonic Axial Flow Turbine With Temperature Distortions

NUMERICAL INVESTIGATION OF THE UNSTEADY FLOWS IN A TRANSONIC AXIAL FLOW TURBINE WITH TEMPERATURE DISTORTIONS

Simone Salvadori[1], Paolo Adami[1], Francesco Martelli[1], Kam S. Chana[2]

[1]Università di Firenze, Dipartimento di Energetica "Sergio Stecco"
via di S. Marta, 3 50139 Firenze, Italy
Contact author: Simone.Salvadori@unifi.it

[2]QinetiQ, Cody Technology Park, Ively Road
Farnborough Hants, GU14 0LX, UK

ABSTRACT

From an industrial point of view, the evaluation of the aero-thermal flow field in the modern gas turbines has grown in importance during the last years. The CFD simulation of the turbine stages can provide numerous information that can be used during the design process to improve the performances and the reliability of the machines. Furthermore, the use of the numerical tools allow the designers to study the effects of different working conditions on the flow field. In particular, the effect of the temperature distortions at the stage inlet on the flow field should be investigated to equip the high pressure stages with adequate cooling systems. The CFD simulation of this kind of test case requires an appropriate unsteady modeling, a high order solution and the use of a suitable turbulence model. A numerical campaign has been conducted by the University of Florence on the QinetiQ's MT1 test case through a series of unsteady simulations performed using the in-house developed CFD code HybFlow. This test case is and un-shrouded, un-cooled high pressure transonic stage with 32 stator and 60 rotor blades that has been experimentally investigated by QinetiQ within the EU funded TATEF and TATEF2 projects. Four different inlet conditions have been simulated: for a uniform total pressure field a uniform and three non-uniform total temperature distributions have been imposed according to the experimental analysis. Amongst the non-uniform distributions, two of them show the same temperature field and are used to study the clocking effects aligning the hot spot to the vane and the blade leading edge. Numerical results obtained using the unsteady method have been compared with experimental data, focusing on the stator-rotor interaction features. The differences in terms of performance parameters and hot fluid redistribution, as well as unsteady fluctuations on the end-walls, have been underlined. Special attention has been paid on the rotor blade pressure and heat transfer rate distributions.

NOMENCLATURE

C	Chord [m]
k	Turbulent kinetic energy [m^2/s^2]
k_{fc}	Fluid conductivity [W/(m K)]
h_c	Convective heat transfer coefficient [$W/(m^2 K)$]
l	Characteristic length [m]
L	Turbulent length scale [m]
Nu	Nusselt number [-]
$\dot{q}$	Heat transfer rate [W/m^2]
T	Total temperature [K]
Tu	Turbulence intensity level [-]

x	Axial coordinate [m]
y^+	y plus

GREEK

ω	Dissipation of k [1/s]

SUBSCRIPTS

0	total/stagnation value
1	inlet section (turbine stage)
ax	axial
cc	combustion chamber
in	inlet section (combustion chamber)
out	outlet section (combustion chamber)
wall	value on the surface

ABBREVIATIONS

CFD	Computational Fluid Dynamics
MFR	Mass Flow Rate
OTDF	Overall Temperature Distribution Factor

INTRODUCTION

Combustion chamber mean exit temperature values have increased considerably to allow higher efficiency and specific power. This has led to complex cooling designs for high pressure stages of gas turbines to avoid over-heating of stationary and rotating parts. The knowledge of the unsteady thermal field becomes increasingly important, especially in the presence of inlet temperature distortions. During the last 10 years, the knowledge of the unsteady phenomena has improved considerably and some general assumptions have been achieved. The steady pressure field associated to the blade load is a source of unsteadiness for the adjacent rows. This mechanism is purely inviscid and is referenced as "potential". Characteristic frequencies of the unsteady stator/rotor interaction are functions of the shaft rotational velocity and of the blade count. Periodicity of the wake/blade and secondary flow interaction is determined by the working conditions through the stage reduced frequency number, which is defined as the ratio between the main flow-scale divided by the perturbation timescale.

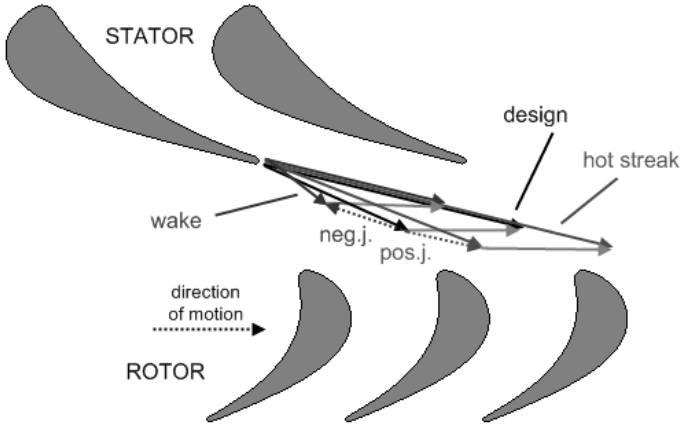

Figure 1. Segregation effect for wakes and hot streaks

The shape of the inlet total temperature field exiting from modern combustion chambers needs to be accounted for. The hot spots entering the stage are convected as hot streaks by the main flow and are redistributed through the "segregation effect" phenomenon described by Kerrebrock and Mikolajczak (1970) (Figure 1). The hot fluid migrates into the stage and tend to accumulate on the rotor pressure side as shown by Butler *et al.* (1989). Furthermore, Shang and Epstein (1997) showed

that the hot fluid moved towards the rotor hub end-wall. All the experimental and numerical analysis that followed the study of Butler confirmed that the segregation effect is the dominant mechanism of redistribution of hot fluid in the rotational frame of reference. A similar behavior can be individuated for the wakes, that are seen as a velocity deficit with respect to the main-flow: the cold fluid moves toward the blade suction side acting like a negative jet and generating a turbulent spot that enhances the boundary layer turbulence level. Studies by Rai and Dring (1990) and Dorney *et al.* (1992) explained that an important mechanism of redistribution of hot streaks is the interaction between segregation effect and passage vortex. Dorney and Gundy-Burlet (1992, 1995) showed that neither hot streaks nor blade metal temperature influences the time-averaged behaviour of isentropic Mach number on the blade surface. Roback and Dring (1992)) showed that aligning the hot spot to the stator leading edge significantly reduces the thermal loads on the rotor blade. The hot fluid moves onto the stator suction side and interacts with the stator wake's negative jet. This interaction weakens the strength of both the segregation effect and results in a more uniform temperature field. This kind of configuration helps rotor surface temperature control but, requires a more in-depth study of stator cooling systems.

To deal with interaction phenomena, several unsteady methods for the numerical simulation of the turbine stage have been proposed. The main problem is represented by the blade count ratio, which impose the spatial periodicity and then the number of blades to be accounted for. The Reduced Count Ratio (RCR) method has been proposed by Dawes (1992) and by Rai and Madavan (1988). Considering a turbine stage with an unfavourable blade count ratio, using this approach the number of the blades is changed to obtain computationally less expensive ratios. The use of this method results in the variation of the blade number and the deterministic frequencies, with the flow characteristics changed. Variation of the throat area of a vane may result in chocking problems in transonic stages. Phase Lag methods avoid the geometrical approximation and propose to use the correlation between the spatial and the temporal periodicity to update the solution in single and multi-row simulations. The first study on this approach has been proposed by Erdos *et al.* (1977), subsequently Koya and Kotate (1985) extended his study to viscous stages and finally He (1992) concluded the development of this phase lag approach. An extended review of the unsteady methods have been performed by Salvadori (2008).

This paper aims to compare the experimental data with the numerical results obtained by the in-house HybFlow CFD code, developed at the Energetic Department of the University of Florence, to assess the CFD capabilities for the investigation of the unsteady interaction in a three-dimensional HP stage with inlet temperature distortions. The experiments are conducted on the MT1 turbine using the QinetiQ turbine facility. Obtained results have been compared with experimental values provided by QinetiQ in the frame of TATEF and TATEF2 EU Framework projects.

Experimental setup and inlet conditions

Measurements have been taken using the QinetiQ Turbine Test Facility (TTF), a short duration wind tunnel for testing full-sized high-pressure turbine stages. The turbine investigated is the MT1 HP stage that is an un-shrouded, high pressure research turbine designed by Rolls-Royce and tested in the turbine facility at QinetiQ. The stage has 32 stator and 60 rotor blades and the nozzle guide vane exit Reynolds number is $2.54*10^6$. The stage has been modelled in its un-cooled configuration and with a rotor tip-gap value of 0.56mm.. Four different total temperature distributions at the stage inlet have been considered to evaluate the impact of the hot fluid on the stationary and rotating walls. The parameter used to catalogue the hot spots is the Overall Temperature Distribution Factor, defined as the difference of the peak and the area-averaged combustor exit temperature, divided by the temperature rise across the combustor:

$$OTDF = \frac{T_{out,cc} - \overline{T}_{out,cc}}{\overline{T}_{out,cc} - \overline{T}_{in,cc}} \tag{1}$$

The test without hot spots has been called OTDF0, the tests with temperature distortion aligned with the vane passage and the vane leading edge have been defined as OTDF1 and OTDF2 respectively while the one with the enhanced profile aligned with the vane leading edge is called OTDFE, as summarized in Figure 2. The shape of the OTDF1 and OTDF2 (on the left) and OTDFE (right) are reported in Figure 2, where the inlet total temperature is divided by the mean inlet total temperature, which is the same for all the cases. The OTDF2 inlet profile has been obtained by rotating the OTDF1 profile by half a stator pitch. The number of hot spots is matched to the number of stators. The measurement plane for the stage inlet An exhaustive description of the temperature distortion generator has been given by Povey *et al.* (2007). For other boundary conditions, all the calculations have been performed at the same uniform total pressure condition at the stage inlet, while the mean static pressure value at the outlet have been imposed coupled with a radial equilibrium condition. The flow at the stage inlet is taken to be axial. The boundary conditions, according to the experimental tests, are reported in Table 2. A large amount of time-resolved results (for the OTDF0 configuration) and time-averaged results (for OTDF1 and OTDF2) has been provided by QinetiQ and University of Oxford (Chana and Mole (2000), Chana *et al.* (2001)). Time-averaged static pressure and Nusselt number distributions on the blades are provided at three radial heights. The unsteady fluctuations on the rotor casing of the static pressure and the Nusselt number are shown. Time-averaged and time-resolved total temperature maps downstream of the rotor trailing edge have been considered.

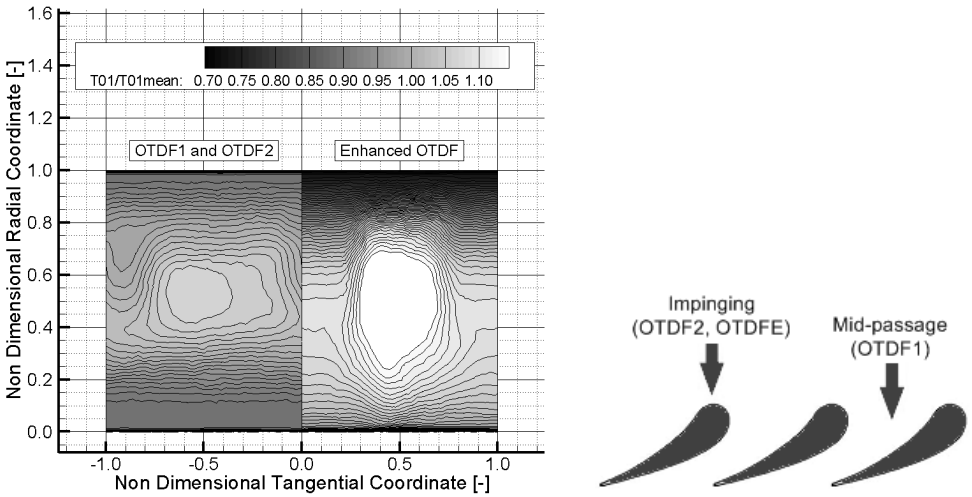

Figure 2. OTDF profiles: contour maps at the stator inlet and impingement position

Table 1 Summary of boundary conditions

Stator Blade Number	32
Inlet Turbulence Level [%]	5.
Inlet Turbulent Length Scale [mm]	0.1
Rotor Blade Number	60
Rotational Speed [RPM]	9500
Non-dimensional Blade Metal Temperature T_{wall}/T_{01mean}	0.65
Non-dimensional Rotor Exit Hub Static Pressure P_3/P_{01mean}	0.32

Numerical approach

The CFD solver HybFlow has already been documented in other works by Adami *et al.* (1998, 2000), then only a brief description is given here. The compressible Navier-Stokes equations are written in the conservative form for a perfect gas. The spatial discretization is based on an upwind Total Variation Diminishing (TVD) finite volume scheme developed for hybrid unstructured grids. Roe's approximate method (Roe (1986)) is used for the upwind scheme and a least-squares linear

reconstruction of the solution inside the elements provides a second order accuracy. Turbulence is modeled using the classical eddy-viscosity assumption through the two equation k-ω model proposed by Wilcox (1994). Inlet conditions are given at the stator entrance imposing the nominal total pressure, total temperature and inlet flow angle. A proper definition of the intensity level Tu and length scale L is used to impose inlet values of k and ω that represent the physical turbulence of the incoming flow. In the exit plane, hub static pressure is imposed based on the experimental data. Pitch-wise radial equilibrium is applied to evaluate the static pressure at other radii. In this regard a fully developed flow field is assumed in the radial equilibrium equation neglecting all axial derivatives.

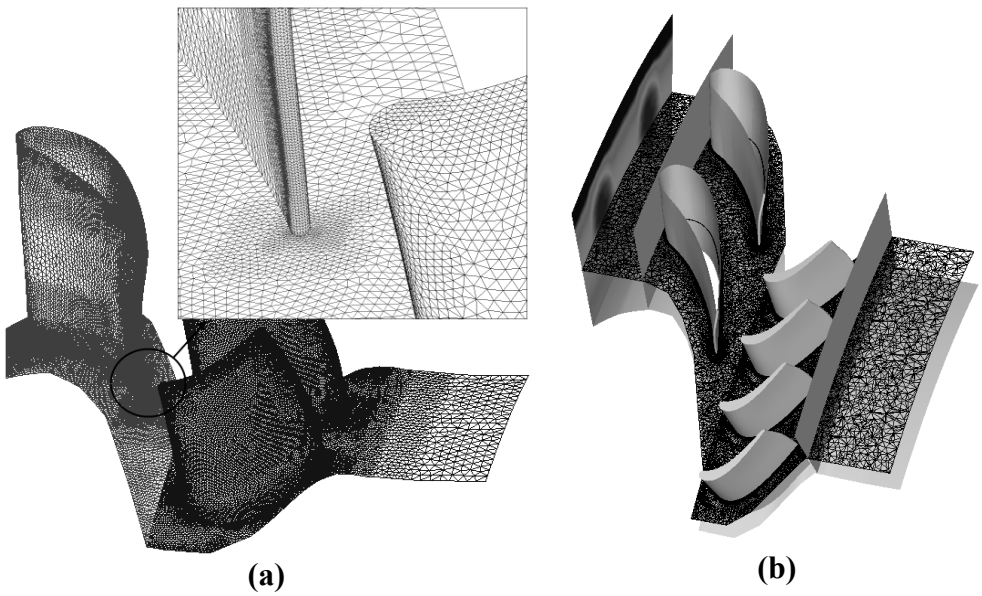

Figure 3. Overview of the mesh (a) and post-processing planes (b)

The hybrid computational mesh is composed of prismatic layers at the solid boundaries and by tetrahedral elements inside the vane. The total amount of elements in the stage computation (one stator and two rotors) is around 3,600,000: amongst them, 1,172,000 have been used for the stator and 1,214,000 for each rotor. Special attention is given to the distance from the wall of the first grid cell, a value of y^+ around 1 is always maintained and, 20 points have been used in the discretization of the boundary layer. Stage unsteady coupling is based on the "reduced count ratio" technique. In the present case the real stator-rotor blade ratio is 32:60 and the nearest periodic ratio of 1:2 has been selected for the simulation. A quasi-homothetic scaling method has therefore been used so that axial length and pitch of the rotor have been reduced to allow the approximated pitch of 1:2 between the rows. The change is applied with scaling of the rotor geometry. Since the mass flow is governed by the chocking of the stator throat, the rotor scaling should not change the design value. Concerning HybFlow, considering the rotational velocity, the vane pitch and the number of numerical passes in which the pitch is divided, the time step used for the calculation is 7.9E-04ms .

Discussion of the obtained results

Discussion of the results obtained is provided through the comparison between the experimental data and the numerical simulations. The frequency range capability of the pressure transducers and the thin film gauges used for the experiments is in the order of 100kHz . The isentropic Mach number and Nusselt number distributions on the blades are illustrated. In addition, the static pressure and heat transfer fluctuations on the rotor casing surface are compared. In Table 2 the performance parameters are reported. As expected, the numerically evaluated mass flow rate is similar in all cases and the value obtained for the OTDF0 configuration is the same as the experiment. In fact, the mean total pressure and total temperature values at the stage inlet remains

the same in the four cases and the stator throat is chocked. This result indicates that the rotor scaling does not generate its chocking.

In Table 2 the total-to-total efficiency of the stage, calculated using the area-weighted values of the total enthalpy at the rows inlet and outlet sections, is also reported. When comparing the results obtained in the nominal case OTDF0 with the experimental data (87.8%), it can be evidenced that CFD underestimates the global efficiency. The uncertainty on the efficiency evaluation is around ± 0.3%, then the CFD result falls out from the experimental range. The under-prediction is caused by the fully turbulent nature of the k-ω turbulence model that neglect the laminar-turbulent transition on the stator blades and enhances the profile losses. This can be proved looking at the loss coefficients of the single row. The value obtained for the stator row is slightly higher than the one obtained for the rotor, while the opposite result were expected. Looking at the results obtained for the OTDFE, an efficiency value higher has been calculated. In this case the loss coefficient for the stator blade is lower than for the other cases and a more detailed analysis is necessary to understand the link between the inlet temperature profile and the resulting better performance.

Table 2. OTDF conditions, MFR and efficiency

	Hot spot position	Non-dimensional MFR	Efficiency
OTDF0	Uniform profile	1.000	86.6%
OTDF1	Vane passage	1.007	86.7%
OTDF2	Vane leading edge	1.009	86.7%
OTDFE	Vane leading dege	1.003	89.6%

Isentropic Mach number on the Blade Surfaces

The experimental and numerical isentropic Mach number and static pressure distributions at mid-span of the stator and rotor blades are reported in Figure 4 and Figure 5. The experimental data are relative to the OTDF0 configuration only. The effect of the OTDF1 or OTDF2 profile on the time-averaged stator and rotor load is not clearly visible. This result was expected on the stator for the OTDF1 profile, since the hot spot is aligned with the vane, but studying the results it seems that aligning the non-uniformity to the blade does not affect the aerodynamic behaviour. This is confirmed by the results obtained in the OTDFE configuration at the mid-span of the stator. It can be concluded that the aerodynamic behaviour on the stator blade is not affected by the inlet temperature profile. The same results have been shown by Gundy-Burlet and Dorney (1997).

From a numerical point of view, the stator load seems to be affected by the unsteady interaction method used in the simulation. In fact, results obtained experimentally differ from the prediction of HybFlow between 70% and 90% of stator profile axial chord. HybFlow shows an under-prediction of the maximum acceleration on the stator suction side. This difference can be related with the inter-stage static pressure value, which was over-predicted. As the rotor geometry has been modified in the unsteady approach, the inter-stage pressure does not match the experimental values. It is interesting to note that the prediction of the suction side acceleration was found to be reasonable near the blade tip, where the scaling has a lower impact on the rotor thickness-to-pitch ratio.

A more detailed analysis of the results obtained on the rotor blade can be carried out. In Figure 4b the time-averaged static pressure distributions at the mid-span of the rotor blade are reported. The lack of agreement of the experimental profiles has already been discussed by Adami *et al.* (2006) and is related to the redistribution of the total blade load on a higher number of blades due to the domain scaling approach. More precisely, the rotor blade load appears to be reduced in the computation as a consequence of the increased number of rotor blades needed for an exact count ratio in the sliding plane treatment. In fact, the experimental and numerical blade load at mid-span have been evaluated and their ratio is the same of the scaling ratio 64:60. Then, the total blade load remains the same but is redistributed over a higher blade number. This change also affects the inter-stage static pressure, which is under-estimated, and the flow acceleration on the rotor blade, which

is under predicted. The effects of the unsteady model on the numerical solution is evidenced by the results obtained by ONERA reported in Figure 5a. The elsA CFD code resolve the stator/rotor interaction using a phase lag approach, allowing a single passage solution for multi-row configurations. As visible, a more accurate evaluation of the time-averaged acceleration of the flow on the suction side is obtained. The results obtained on the pressure side are more accurate than the data obtained by HybFlow and the inter-stage mean static pressure matches the experimental value.

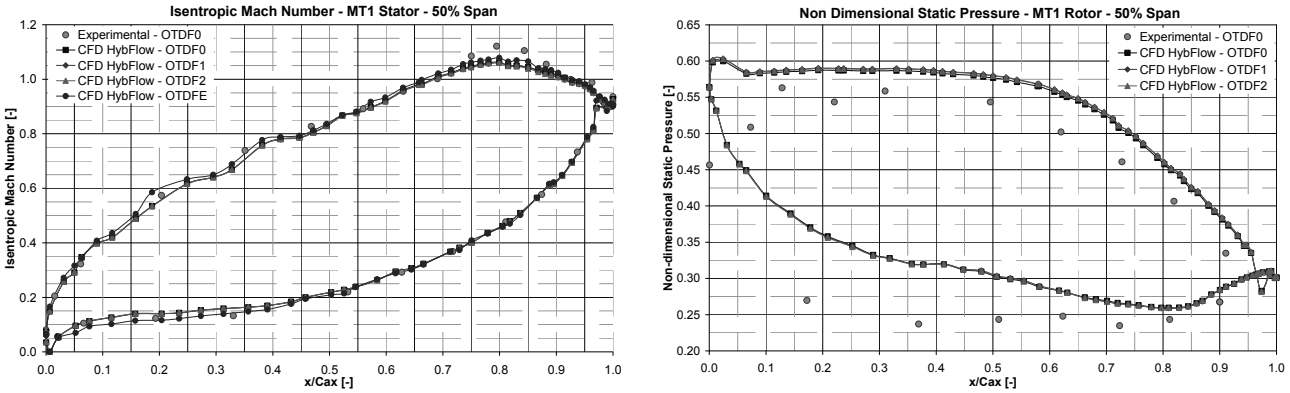

(a) **(b)**

Figure 4. Aerodynamic behaviour on the stator and rotor blades

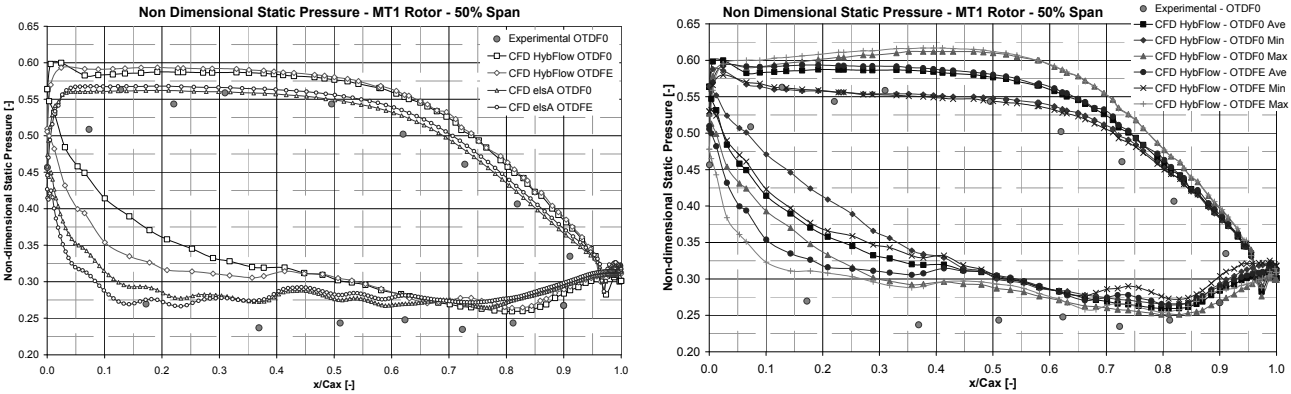

(a) **(b)**

Figure 5 Effects of the OTDFE profile on the rotor pressure distribution

Considering the OTDFE case, a more pronounced acceleration on the rotor suction side is visible in the CFD simulation while the pressure side behaviour remains unchanged. This deviation from the OTDF0 case is explained according to the Munk and Prim's substitution principle (1947). The stator vane, having a uniform total pressure and a non-uniform total temperature field on the inlet, redistributes the hot fluid mainly due to the diffusive terms. The hot fluid entering the stage is, mainly, convected through the low momentum stator blade suction side boundary layer (Roback and Dring (1992)) and, at the interface maintains its tangential non-uniformity. At the stator exit the non-uniform distribution of velocity field is related to the total temperature field. As a consequence, the hot fluid has a greater velocity value than the cold one, but with the same yaw angle. For the rotational frame of reference, a positive jet like effect occurs (Kerrebrock and Mikolajczak (1970)) on the hot flow entering into the rotor passage, as can be seen in the schematic representation reported in Figure 1. This phenomenon explains the expected higher acceleration captured by the CFD simulation. The elsA calculation confirms the higher acceleration of the flow on the suction side due to the positive jet effect (Figure 5a).

A more detailed analysis of the OTDFE effect on the blade load can be performed looking at Figure 5b, where the time-resolved data are reported considering the maximum and minimum blade loads. It can be underlined that the flow behavior on the pressure side is not affected by the

presence of the hot spot. On the suction side, the clocking effects are more pronounced. For the uniform case, the negative jet effect is visible when considering the minimum load profile, with a very weak acceleration of the flow on the suction side. Considering the OTDFE case, the hot fluid interacts with the wake since the hot spot is aligned with the blade. Nevertheless, the positive jet effect is clearly visible as well as a clocking position where the blade load is reduced. This last is not caused by the wake but is relative to the "cold" fluid arriving from the mid-passage.

The OTDF1 and OTDF2 cases do not show any positive incidence effect. In the second case (OTDF2) one can assume that the positive incidence is somewhat balanced by the wake negative incidence effect. The OTDF1 case has the hot spot aligned with the stator vane passage and should show some differences as no wake interaction is expected. From these observations it is concluded that the hot streak intensity for these cases is too weak and the tangential non-uniformity is mixed out at the stage interface, at least in the present CFD simulations.

Heat Transfer Rate on the Blade Surfaces

In Figures from 5 to 9 the time-averaged Nusselt number distributions on the stator and rotor blades are reported. The Nusselt numbers have been calculated as shown in Equation 2. The value of the thermal conductivity k_{fc} has been obtained by an empirical correlation as function of the total temperature (Adami *et al.* (2006)). For the stator blade the total temperatures are absolute and the true chord is taken for the stator, while in the rotor row the relative total temperature and the rotor true chord have been used:

$$Nu = \frac{h_c \cdot l}{k_{fc}} = \frac{\dot{q} \cdot C}{\left(\overline{T}_{01} - T_{wall}\right) \cdot k_{fc}} \tag{2}$$

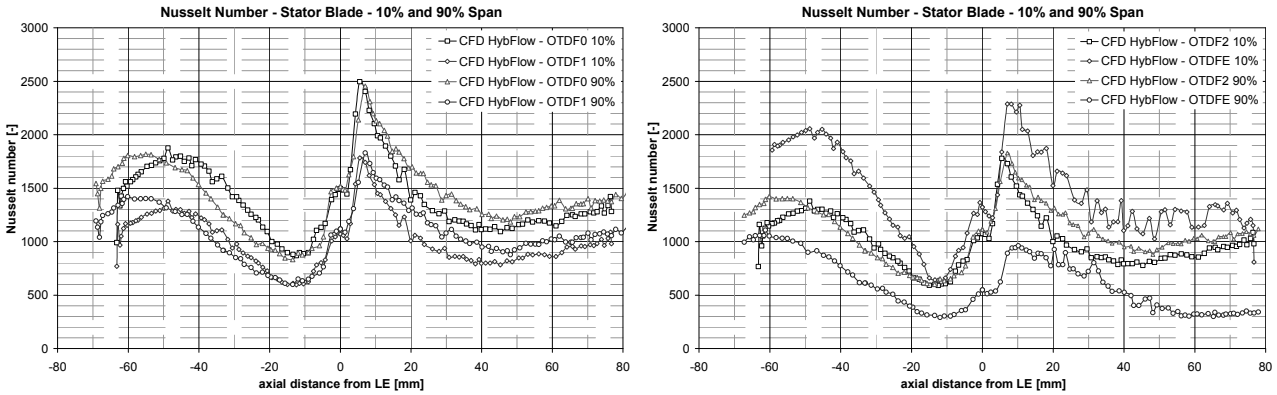

Figure 6. *Nu* number – Stator 10% and 90% (pres. side negative)

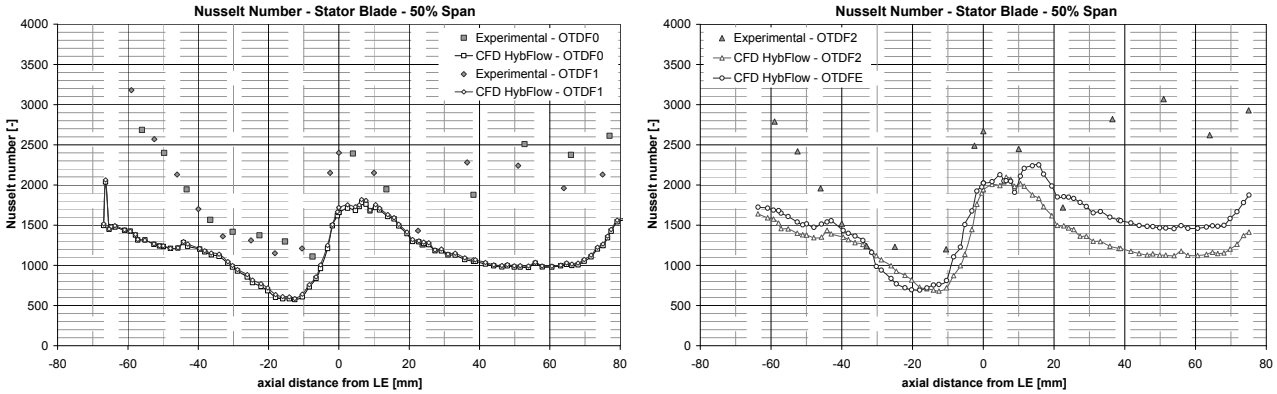

Figure 7. *Nu* number – Stator 50% (pres. side negative)

In Figure 6 and Figure 7 the obtained results for the stator blade at three blade heights are reported. Near the end-walls the OTDF1 configuration show much lower values than the ones

obtained for the OTDF0 configuration. This is consistent with the temperature distribution shown in Figure 2: the temperature level in the zone near the 10% and 90% of the blade span for the OTDF1 profile is lower than the mean value used for the OTDF0 case. At the 50% span the effect of the OTDF2 and OTDFE profiles is clearly visible (Figure 7). On the contrary, it seems that no difference exists between the OTDF0 and the OTDF1 configuration, while the other two boundary conditions generate a higher heat transfer level especially on the suction side, where the hot fluid is principally convected. The differences in heat transfer evaluation on the suction side at 50% span may be attributed to the turbulence modelling, since HybFlow uses the original k-ω model by Wilcox (1994) which is dependent on the far field dissipation rate value and leads to the over-prediction of the eddy viscosity coefficient typical of the two-equation models. The OTDF0 condition is the worst one for the zones near the hub and casing, while special attention on the cooling system design should be addressed when the inlet profile is similar to OTDF2 and OTDFE.

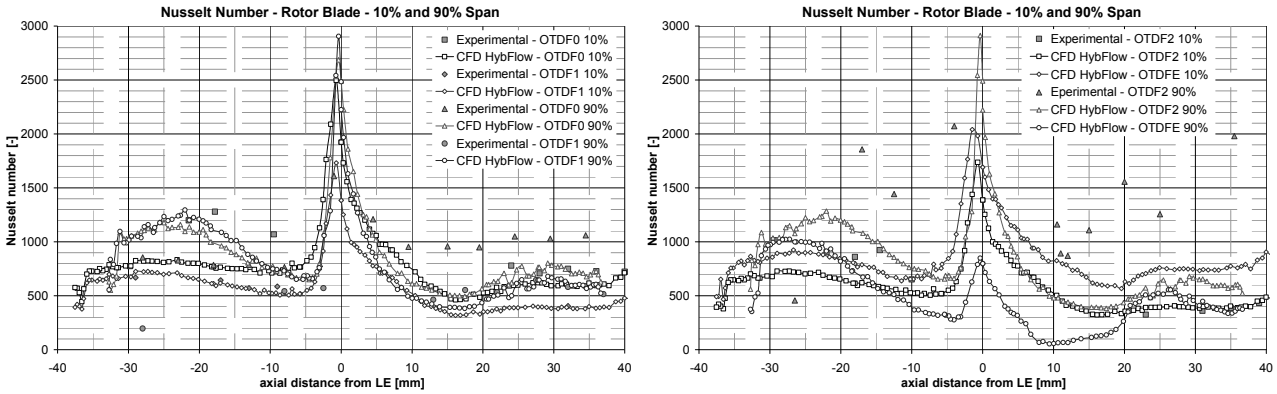

Figure 8. *Nu* number – Rotor 10% and 90% (pres. side negative)

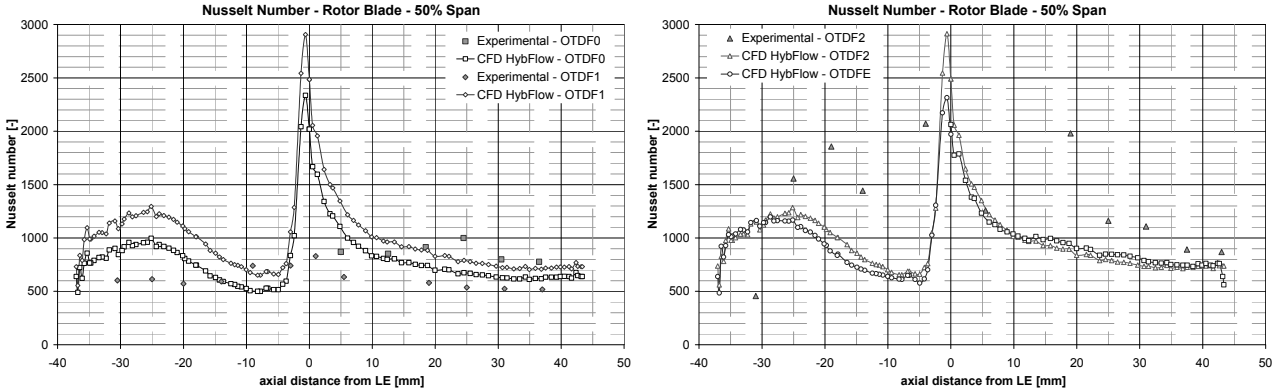

Figure 9. *Nu* number – Rotor 50% (pres. side negative)

In Figure 8 and Figure 9 the Nusselt number on the rotor blade is illustrated. In this case a better agreement between HybFlow and the experiments is visible. At 50% span (Figure 9), looking at the results obtained for the OTDF0 and OTDF1 configurations, the interaction between the passage vortex and the segregation effect is visible. The hot fluid tends to move toward the pressure side of the blade for the positive jet phenomenon and the *Nu* number values obtained for the OTDF1 case are higher the on the pressure side. This effect is enhanced by the passage vortex at the mid-span. In fact, OTDF1 and OTDF2 configurations lead to *Nu* number values on the pressure side that are higher than the ones obtained with the OTDF0 configuration, but at the 50% of the stator blade there were no differences between OTDF0 and OTDF1. A more detailed analysis of the obtained data should be performed to understand the behaviour on the suction side, where the trend in *Nu* between OTDF0 and OTDF1 is opposite when comparing experimental and numerical data. An interesting result concerning the OTDFE case is that its effect on the heat transfer at the mid-span is not different from the one produced by the OTDF2 case, which has a lower peak temperature value. This is not coherent with the aerodynamic results at the 50% rotor span, where the effect of the

positive incidence is visible. One can conclude that initially the hot fluid does not interact with the stator wake and the positive incidence effect is maintained, while in the rotor vane the slip velocity component which moves the hot fluid toward the pressure side is weakened by the wake negative jet. The strength of this interaction depends on the difference between the wake velocity deficit and the hot fluid velocity modulus enhancement.

Pressure and Heat Transfer Fluctuations on the Casing

In Figure 10a and Figure 10b the position of the pressure transducers and the thin film gauges on the over-tip region of the rotor casing are reported. The time-averaged and time-varying static pressure was measured on the rotor casing using 57 flush-mounted pneumatic tappings and high-frequency response miniature pressure transducers (Kulites). The Kulites were mounted in the same locations as the pneumatic tappings. The transducers were fitted in rows at an angle of 52 deg to the axial plane, approximately following the stagger angle of the rotor blade. In and Figure 10c and Figure 10d the time resolved non-dimensional pressure fluctuations calculated with respect to the time-mean pressure values are reported for points 7 and 17. Considering the experimental data relative to the OTDF0 case, there is a satisfactory agreement between the numerical data and the experiments for all the considered gauge locations.

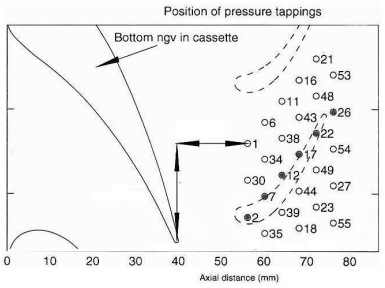

(a) Pressure probes

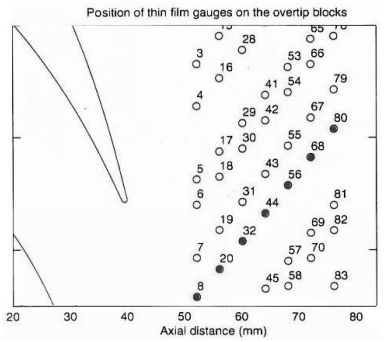

(b) Thin film gauges

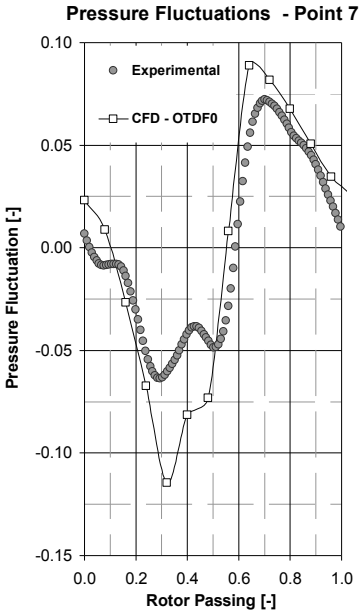

(c) Point 7

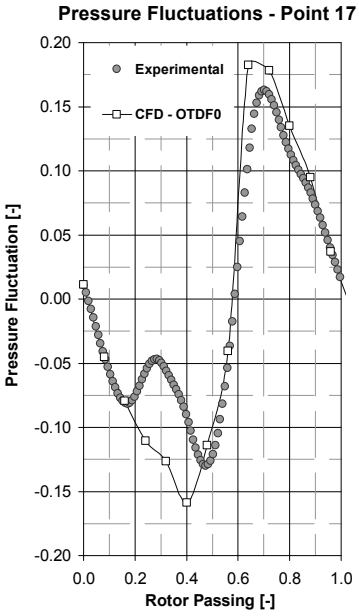

(d) Point 17

Figure 10. Pressure and heat transfer probes position and fluctuations in points P7 and P17

The numerical simulation does not reproduce exactly the minor fluctuations produced by the presence of the tip leakage vortex, which generates a first compression followed by the one generated by the blade passage itself under the pressure transducer location. This mechanism is more pronounced at the mid-chord, where the vortex is more developed. Looking at Figure 11, it can be evidenced that the effect of the inlet total temperature distortion is negligible considering the pressure field on the casing. This is an expected behaviour since the hot streak redistribution in the rotor row is governed by the segregation effect which is essentially limited to the blade mid-span for the inlet temperature profiles. Furthermore, the hot fluid tends to move toward the platform and then the flow near the tip of the blade is mainly governed by the pressure gradient between the rotor blade sides and the tip-casing gap dimension. In Figure 11 the fluctuations of the Nusselt number evaluated on the rotor casing in the tip region are also reported for point 32 and 56, which position corresponds to the one of the pressure transducers 7 and 17. The amplitude of the oscillation does not reproduce the experimental one especially for point 32. Considering the numerical data. the

presence of a tangential non-uniformity does not seem to affect the heat transfer on the over-tip region. In fact, all the computations show nearly the same amplitude and the same oscillation frequencies. Comparing the data reported in Figure 11 we note that the Nusselt number fluctuations are connected to the pressure fluctuations. The heat transfer rise which is visible between 0.6 and 0.9 rotor passages is therefore a function of the compression of the leakage flow in the over-tip region. This conclusion is coherent with the results shown by Thorpe *et al.* (2007).

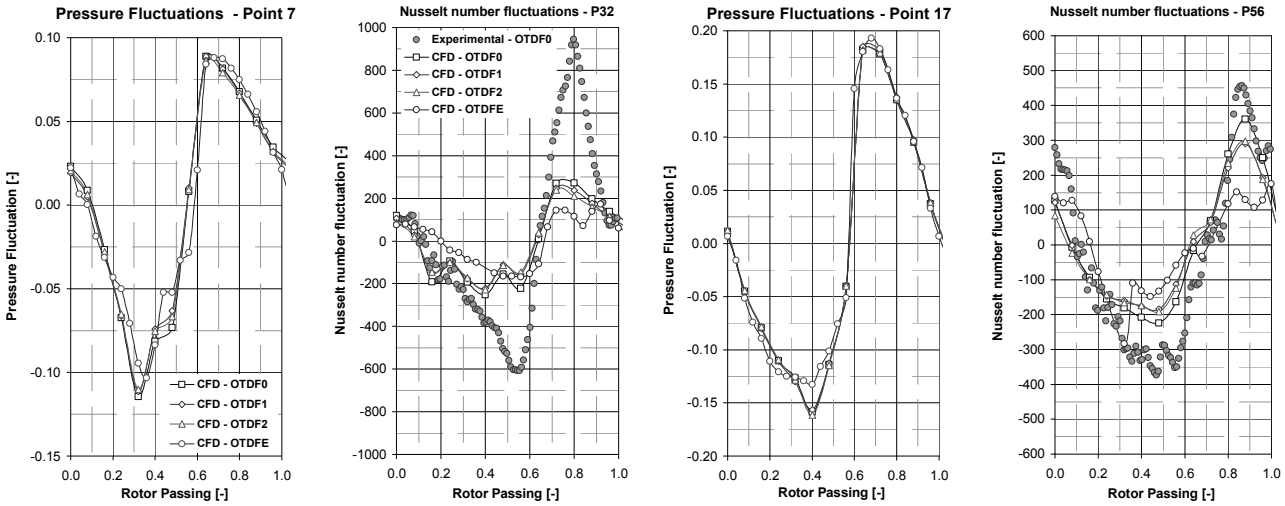

(a) P7-HT32 **(b) P17-HT56**

Figure 11. Pressure fluctuation in the points P7-HT32 and P17-HT56

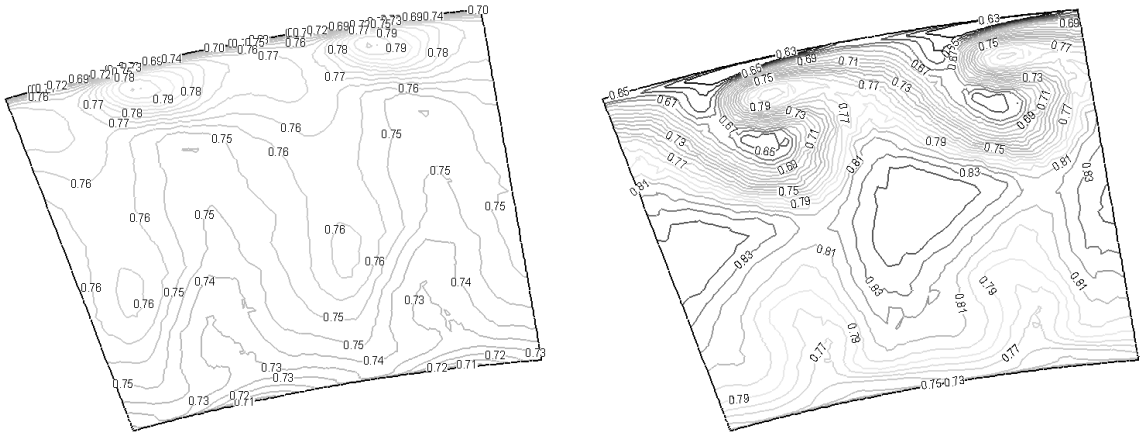

Uniform inlet **Enhanced OTDF**

Figure 12 Non dimensional time-averaged absolute total temperature

"Near Plane" downstream of the rotor row

The time-averaged and time-resolved absolute total temperature profiles on a plane located 0.33 axial chords downstream of the rotor trailing edge have been compared with each other. In Figure 12 the time-averaged values obtained for the uniform and enhanced inlet conditions are reported. As visible, the profiles are very different in shape and levels. Considering the OTDF0 case, the temperatures are limited between 0.73 to 0.78 over almost all the plane while the range that is obtained for the OTDFE case is much wider. Furthermore, it must be underlined that at the stage exit some temperature hot spots can be individuated, which intensity is only 15% lower than the mean stage inlet value. Therefore the hot fluid redistribution is not limited to the first turbine stage but attention should be given to the evaluation of the heat load on the second stage stator. Furthermore, it can be observed that the high temperature regions are quite balanced between 40% and 60% of the span with slightly higher values under the 50%. This is coherent with the results showed by Shang and Epstein (1997), where the hot fluid tends to move toward the rotor platform.

The time-resolved absolute total temperature profiles at mid-span are reported in Figure 13. As visible, in the OTDFE case white zones indicate the approaching of a hot spot which intensity is 89% of the mean inlet temperature. This temperature non-uniformity should not be neglected when considering the successive turbine stages, which are then subjected to temperature non-uniformities of high intensity. Furthermore, it can be observed that for OTDF1 and OTDF2 cases the inlet temperature condition generates temperature levels which are higher than the OTDF0 case. Furthermore, the hot core seems to be positioned in different tangential positions and instants: (0.8, 0.2) for the OTDF1 and around (0.6, 0.4) for OTDF2. This is caused by the different clocking of the hot spot at the stage inlet: considering the OTDFE case the hot core is positioned as for the OTDF2 case and both the cases have the inlet non-uniformity aligned with the stator leading edge.

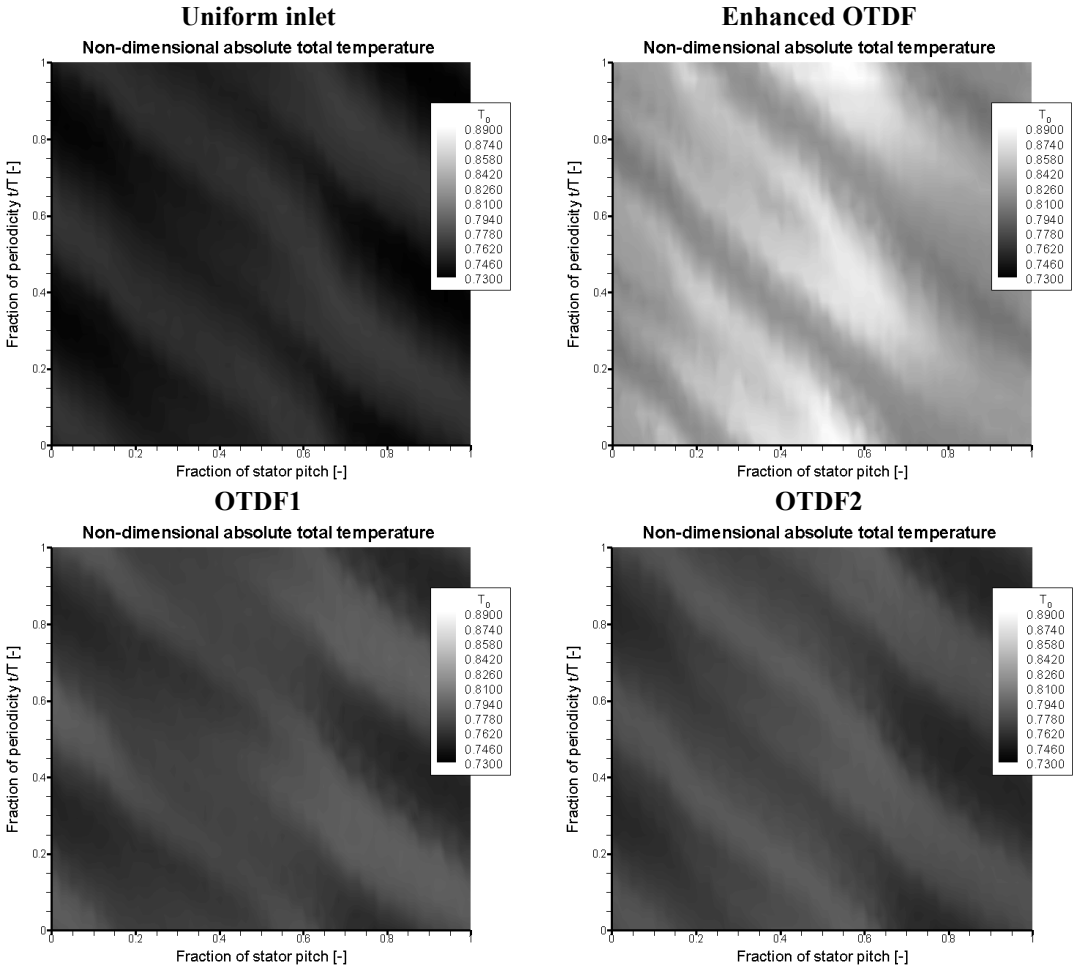

Figure 13 Non dimensional time-resolved absolute total temperature at mid-span

Conclusions

The effects of several inlet temperature profiles on the aero-thermal flow field of the MT1 high pressure turbine stage have been analyzed. Numerical results have been analyzed and compared with the experimental data from QinetiQ. The following conclusions can be summarized:

- The use of a domain scaling approach for the unsteady simulation causes an underestimation of the time averaged rotor blade load and modifies the potential interaction effects.
- An enhanced inlet temperature distortion aligned with the stator leading edge affect appreciably the rotor aerodynamics.
- The rotor casing heat transfer fluctuations are in sympathy with the pressure ones.
- In presence of inlet temperature non-uniformities, the hot spots are not limited to the first turbine stage but can be observed at the stage exit, too, affecting the second stage heat load.

Acknowledgments

The European Commission and the European manufacturers are acknowledged for the permission to use the data obtained in the frame of the EU funded TATEF (Turbine Aero-Thermal External Flows) and TATEF2 projects. The authors would like to acknowledge Dr. F. Montomoli for the support provided during the CFD simulation of the test cases. The authors would also like to acknowledge Dr. T. Povey from Oxford University for the permission to use the TATEF2 preliminary "Enhanced OTDF" profile, and Dr. L. Castillon from ONERA for the permission to use the numerical data.

References

[1] J.L. Kerrebrock, A.A. Mikolajczak, 1970, *Intra-Stator Transport of Rotor Wakes and Its Effects on Compressor Performance*, *J. Eng. P.*, vol. 92, no. 4, pp. 359-368

[2] T.L. Butler, O.P. Sharma, H.D. Joslyn, R.P. Dring, 1989, *Redistribution of an Inlet Temperature Distortion in an Axial Flow Turbine Stage*, *AIAA J. Propul. Power*, vol. 5, pp. 64-71

[3] T. Shang, A.H. Epstein, 1997, *Analysis of Hot Streak Effects on Turbine Rotor Heat Load*, *ASME J. Turbomach.*, vol. 119, pp. 544-553

[4] M.M. Rai, R.P. Dring, 1990, *Navier-Stokes Analysis of the Redistribution of Inlet Temperature Distortion in a Turbine*, *AIAA J. Propul. Power*, vol. 6, no. 3, pp. 276-282

[5] D.J. Dorney, R.L. Davis, D.E. Edwards, N.K. Madavan, 1992, *Unsteady Analysis of Hot Streak Migration in a Turbine Stage*, *AIAA J. Propul. Power*, vol. 8, no. 2, pp. 520-529

[6] D.J. Dorney, K.L. Gundy-Burlet, 1995, *Hot-Streak Clocking Effects in a 1-1/2 Stage Turbine*, *AIAA J. Propul. Power*, vol. 12, no. 3, pp. 619-620

[7] K.L. Gundy-Burlet, D.J. Dorney, 1997, *Influence of 3D Hot Streaks on Turbine Heat Transfer*, *Int. J. Turbo Jet Eng.*, vol. 14, pp. 123-131

[8] R.J. Roback, R.P. Dring, 1992, *Hot Streaks and Phantom Cooling in a Turbine Rotor Passage. Part II – Combined Effects and Analytical Modelling*, *ASME J. Turbomach.*, vol. 115, pp. 667-676

[9] S. Salvadori, 2008, *Numerical Investigation of the Unsteady Flows and Heat Transfer in the High Pressure Gas Turbine Stages*, Doctoral These, University of Florence, Italy

[10] W.N. Dawes, 1992, *The Simulation of Three-Dimensional Viscous Flow in Turbomachinery Geometries Using a Solution-Adaptive Unstructured Mesh Methodology*, *ASME J. Turbomach.*, vol. 114, no 3, pp. 528-537

[11] M.M. Rai, N.K. Madavan, 1988, *Multi-Airfoil Navier-Stokes Simulations of Turbine Rotor-Stator Interaction*, Proc. Of the AIAA Aerospace Sciences Meeting, 26th, Reno, Nevada (USA), Jan 11-14, AIAA-1988-361

[12] J.I. Erdos, E. Alzner, W. McNally, 1977, *Numerical Solution of Periodic Transonic Flows through a Fan Stage*, *AIAA J.*, vol. 15, pp. 1559-1568

[13] M. Koya S. Kotake 1985, *Numerical Analysis of Fully Three-Dimensional Periodic Flows Through a Turbine Stage*, *J. Eng. Gas Turb. Power*, vol. 107, pp.945-952

[14] L. He, 1992, *Method of Simulating Unsteady Turbomachinery Flows with Multiple Perturbations*, *AIAA Journal*, vol. 30, pp. 2730-2735

[15] T. Povey, K.S. Chana, T.V. Jones, J. Hurrion, 2007, *The effect of Hot-Streak on HP Vane Surface and Endwall Heat Transfer: an Experimental and Numerical Study*, *ASME J. Turbomach.*, vol. 129, pp. 32-43

[16] K.S. Chana, A.H. Mole, 2000, *A Summary of Cooled NGV and Un-Cooled Rotor Measurements from the MT1 Single Stage High Pressure Turbine in the DERA Isentropic Light Piston Facility (UL)*, TATEF Project (BRPR-CT97-0519)

[17] K.S. Chana, T. Patel, A.H., Mole, 2001, *A Summary of Measurements with a Non-Uniform Inlet Temperature Profile from the MT1 Single Stage HP Turbine,* TATEF Project (BRPR-CT97-0519)

[18] P. Adami, V. Michelassi, F. Martelli, 1998, *Performances of a Newton-Krylov Scheme against Implicit and Multi-Grid Solvers for Inviscid Flows*, AIAA Paper 98-2429

[19] P. Adami, F. Martelli, V. Michelassi, 2000, *Three-Dimensional Investigations for Axial Turbines by an Implicit Unstructured Multi-Block Flow Solver*, *Proc. of the ASME IGTI Turbo Expo 2000*, Munich, Germany, May 8-11, ASME 2000-GT-0636

[20] P.L. Roe, 1986, *Characteristic based scheme for Euler equations*, *Ann. Rev. Fluid Mech.*, vol. 18, 337-365

[21] D.C. Wilcox, 1994, *Simulation of Transition with a Two-Equation Turbulence Model*, *AIAA J.*, vol. 32, no. 2

[22] P. Adami, S. Salvadori, K.S. Chana, 2006, *Unsteady Heat Transfer Topics in Gas Turbine Stages Simulations, Proc. of the ASME IGTI Turbo Expo 2006*, Barcelona, Spain, May 8-11, ASME GT2006-90298

[23] M. Munk, R. Prim, 1947, *On the Multiplicity of Steady Gas Flows having the Same Streamline Patterns*, *Proceedings of the National Academy of Science*, vol. 33, pp. 137-141

[24] S.J. Thorpe, R.J. Miller, S. Yoshino, R.W. Ainsworth, N.W. Harvey, 2007, *The Effect of Work Processes on the Casing Heat Transfer of a Transonic Turbine*, *J. Turbomach.*, vol. 129, pp. 84-91